

## Observation of strong electron-phonon coupling effects in YbPO<sub>4</sub>

P. C. Becker,\* G. M. Williams<sup>†</sup>, and N. M. Edelstein

*Materials and Chemical Sciences Division, Lawrence Berkeley Laboratory, Berkeley, California 94720*

J. A. Koningstein

*Department of Chemistry, Carleton University, Ottawa, Ontario, Canada*

L. A. Boatner and M. M. Abraham

*Solid State Division, Oak Ridge National Laboratory, Oak Ridge, Tennessee 37830*

(Received 29 May 1991)

The electronic and vibrational Raman spectra of a single crystal of YbPO<sub>4</sub> have been investigated. The  $E_g$  phonon at 310 cm<sup>-1</sup> is found to have an anomalously large Raman linewidth of 50 cm<sup>-1</sup> at room temperature. Particularly striking was the observation that this transition is split into several separate transitions that move apart in energy as the temperature is lowered. The magnitude of these effects is very large. These observations are interpreted on the basis of electron-phonon coupling, and phenomenological calculations are presented and compared with the experimental data.

Coupling between the electronic states of rare-earth ions doped in a crystal and the vibrational modes of the lattice are usually weak due to the effective shielding of the 4*f* electrons of the rare-earth ions. In the present work surprising results are presented for the system YbPO<sub>4</sub>, which shows a temperature-dependent electron-phonon coupling with coupling strengths an order of magnitude larger than any previously reported.<sup>1-10</sup> The effect is observed using electronic Raman spectroscopy, which uncovers in a precise fashion the character of the low-lying energy states.<sup>11-14</sup> The underlying cause of the anomalously large electron-phonon coupling effects is not understood, nor is it clear why the effect is restricted to the ytterbium ion. Phenomenological calculations, based on the low-lying energy level structure of Yb<sup>3+</sup>, are presented, which qualitatively account for the temperature dependence of the splitting of the  $E_g$  phonon at 310 cm<sup>-1</sup>. The effects reported here should have implications for the physics of electron-phonon coupling in rare-earth systems.

The rare-earth phosphate systems have been the object of several magnetic and optical studies.<sup>15,16</sup> Studies of electronic Raman scattering in ErPO<sub>4</sub> and TmPO<sub>4</sub>, which are isostructural with YbPO<sub>4</sub>, have been reported previously, and these results show no strong evidence of electron-phonon coupling.<sup>12</sup>

At room temperature, the Raman spectra of the rare-earth phosphate crystals consist only of the vibrational spectrum of the lattice. The phonons are described by the irreducible representations of the group  $D_{4h}$ . At low temperatures ( $T < 80$  K), the phonon peaks narrow slightly and shift by a few wave numbers and new peaks appear which correspond to the electronic Raman transitions of the rare-earth ion.<sup>11-14</sup> For TmPO<sub>4</sub> and ErPO<sub>4</sub>, the electronic Raman peaks appear at the positions predicted by the absorption spectra and the crystal-field fits.<sup>12</sup> The vibrational spectrum contains a very strong

phonon peak of symmetry  $E_g$  (labeled  $E_g^3$  in the figures, as in Ref. 14) at about 310 cm<sup>-1</sup>.

Figure 1 shows the Raman transitions in the 310-cm<sup>-1</sup> spectral region for LuPO<sub>4</sub>, TmPO<sub>4</sub>, and YbPO<sub>4</sub> at room temperature and at  $T=4.2$  K. As shown in Fig. 1, for crystals such as LuPO<sub>4</sub> and TmPO<sub>4</sub> the linewidth of this peak is about 8 cm<sup>-1</sup> at room temperature and narrows to 4 cm<sup>-1</sup> at  $T=4.2$  K (the spectral bandpass of the spectrometer used was 2.5 cm<sup>-1</sup>). A peak at the expected location of  $E_g^3$  also appears in the room-temperature Raman spectrum of YbPO<sub>4</sub> with an asymmetrical line shape and an anomalously large linewidth of approximately 50 cm<sup>-1</sup>. As the sample is cooled to  $T=4.2$  K the peak does not narrow but, instead, splits into two sharp "wings" plus a broad central feature, spanning a spectral region of almost 100 cm<sup>-1</sup>.

The temperature evolution of the  $Y(XZ)X$  spectrum of YbPO<sub>4</sub> in the 250–350-cm<sup>-1</sup> region is shown in Fig. 2 [see footnote 25 of Ref. 12 for the definition of the nomenclature  $Y(XZ)X$ ]. For this polarization configuration, the phonons observed are of  $E_g$  symmetry, and the symmetry of the electronic transitions observed is  $\Gamma_5$  (or  $E$ ). A fairly smooth transition is observed between the room temperature and  $T=4.2$  K spectra. At  $T=4.2$  K, the two sharp peaks are at roughly 248 and 344 cm<sup>-1</sup>, symmetrically placed with respect to the original room-temperature peak. The broad central feature is at about 298 cm<sup>-1</sup>. This splitting cannot be explained as arising from a static cooperative Jahn-Teller effect as observed in other rare-earth zircon systems.<sup>17,18</sup> Indeed, none of the other  $E_g$  phonons show any anomalous linewidths, nor do any of them split into two components as the temperature is decreased.

YbPO<sub>4</sub> has the zircon structure with Yb<sup>3+</sup> at a site of  $D_{2d}$  symmetry. Two ions, related by a center of inversion, are in the primitive cell which has  $D_{4h}$  symmetry. Yb<sup>3+</sup> has a  $4f^{13}$  configuration (equivalent to a  $4f^{13}$

configuration), so that the electronic energy-level structure simply consists of a  ${}^2F$  manifold which is split by the spin-orbit interaction into a ground  ${}^2F_{7/2}$  term and an excited  ${}^2F_{5/2}$  term at  $10\,000\text{ cm}^{-1}$ . These  $J = \frac{7}{2}$  and  $J = \frac{5}{2}$  levels are further split by the crystal field into 4 and 3 Kramer's doublets, respectively. The total crystal-field splitting of the  $J$  multiplets is approximately  $300\text{ cm}^{-1}$  and is discussed in Ref. 16.

Crystal-field fits of the absorption spectra of  $\text{Yb}^{3+}$  in  $\text{LuPO}_4$  and  $\text{YbPO}_4$  indicate that two of the  $\text{Yb}^{3+}$  ground-state multiplet energy levels are located very close in energy [ $279\text{ cm}^{-1}$  ( $\Gamma_6$ ) and  $289\text{ cm}^{-1}$  ( $\Gamma_7$ )] to the  $E_g^3$  phonon at  $310\text{ cm}^{-1}$ .<sup>16</sup> Coupling between the electronic states and the optical phonon will be reinforced by their near degeneracy, and the true eigenstates of the system in that energy region will have a mixed electronic and vibrational character, as discussed extensively by Schaack and co-workers<sup>1-8</sup> and Thalmeier and Fulde.<sup>9,10</sup> In the case of  $\text{YbPO}_4$ , three modes, two electronic and one vibrational, can participate in the coupling. This

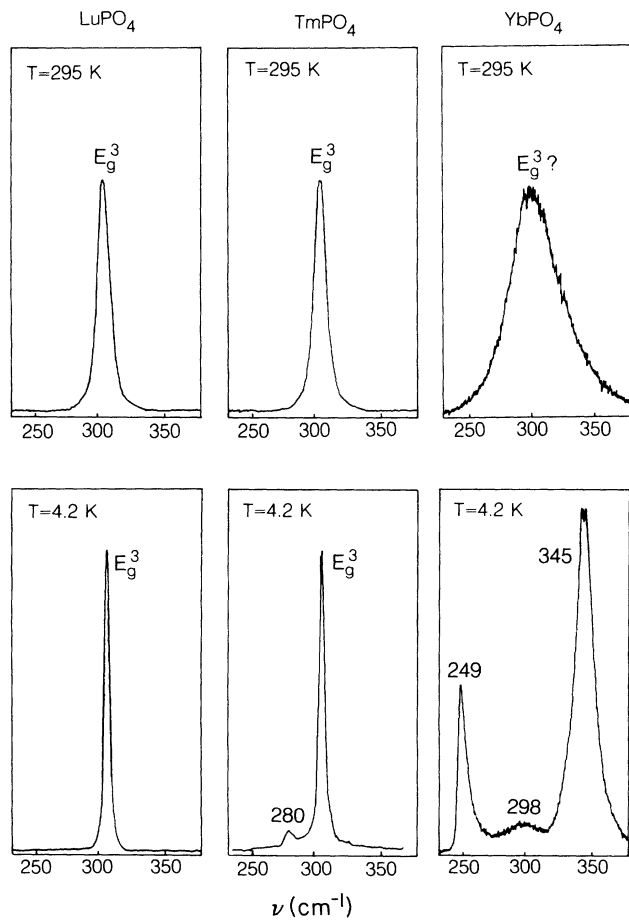


FIG. 1. Raman spectra of the crystals  $\text{LuPO}_4$ ,  $\text{TmPO}_4$ , and  $\text{YbPO}_4$ , at room temperature and 4.2 K, in the  $300\text{-cm}^{-1}$  region. The spectra were taken in the  $Y(XZ)X$  polarization configuration (see footnote 25, Ref. 11 for a definition of the nomenclature). The numbers in the figure are peak positions in  $\text{cm}^{-1}$ . The line at  $280\text{ cm}^{-1}$  in the  $\text{TmPO}_4$   $T=4.2\text{ K}$  spectrum is an electronic Raman transition of  $\text{Tm}^{3+}$ .

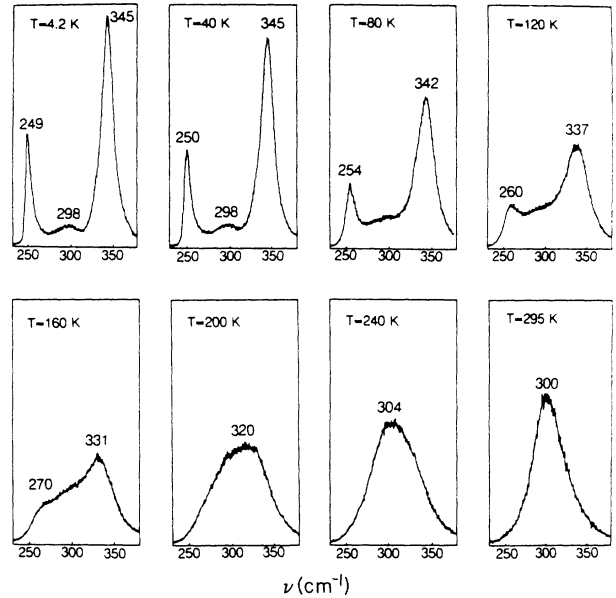


FIG. 2. Raman spectra of the crystal  $\text{YbPO}_4$  in the  $Y(XZ)X$  configuration, in the  $300\text{-cm}^{-1}$  region, as a function of temperature between room temperature and  $T=4.2\text{ K}$ . The numbers in the figures are peak positions in  $\text{cm}^{-1}$ .

would account for the three features in the  $T=4.2\text{ K}$  Raman spectra.

An appropriate way to interpret the coupled-mode spectrum of  $\text{YbPO}_4$  is to use a picture involving excitations rather than energy levels.<sup>19</sup> Two electronic excitations can be coupled with the vibrational one to form the coupled-mode spectrum in the vicinity of  $300\text{ cm}^{-1}$ . The incident light field drives the coupled excitations that are observed nonlinearly via the Raman effect. The electronic Raman transitions between the  $\text{Yb}^{3+}\Gamma_6$  ( $E_{1/2}$ ) ground state and the  $\Gamma_6$  ( $E_{1/2}$ ) excited state are of symmetry  $\Gamma_1 + \Gamma_2 + \Gamma_5$  ( $A_1 + A_2 + E$ ), while the transitions to the  $\Gamma_7$  ( $E_{3/2}$ ) excited state are of symmetry  $\Gamma_3 + \Gamma_4 + \Gamma_5$  ( $B_1 + B_2 + E$ ). The  $\Gamma_5$  electronic excitations are group theoretically allowed to couple to the  $E_g^3$  phonon at  $310\text{ cm}^{-1}$ , this effect being further enhanced by the near resonance in their energies.

An estimate of the respective coupling strengths of the two electronic excitations with the phonon can be made by considering the standard Jahn-Teller-type electron-phonon interaction Hamiltonian, where the interaction is considered to be localized at a particular  $\text{Yb}^{3+}$  site:<sup>2,9,17,18</sup>

$$H_{e-p} = \sum_{\Gamma_i, p} g_{\Gamma_i, p} O_{\Gamma_i, p} Q_{\Gamma_i}, \quad (1)$$

where  $Q_{\Gamma_i, p}$  is the phonon amplitude for the phonon mode  $p$ ,  $\Gamma_i$  denotes the irreducible representations of  $D_{2d}$ ,  $O_{\Gamma_i}$  is an electronic operator of symmetry  $\Gamma_i$ , and the  $g_{\Gamma_i, p}$  are coupling strengths. The interaction can be extended to the level of the primitive cell by summing over the two sites in the primitive cell. For the purpose of the discussion presented here, however, it is sufficient to consider only the local interaction. An  $E_g$  phonon in-

duces a local distortion of symmetry  $\Gamma_5(E)$  at the  $\text{Yb}^{3+}$  site. Keeping only the doubly-degenerate irreducible representations  $\Gamma_5$ , since the coupled-mode pattern appears in that symmetry, we have  $O_{\Gamma_{5X}} = J_x J_z + J_z J_x$  and  $O_{\Gamma_{5Y}} = J_y J_z + J_z J_y$ , where, for simplicity, only the quadrupolar operators have been retained. Using the wave functions of Ref. 16 we calculate that the transitions at 279 and 289  $\text{cm}^{-1}$  have electron-phonon coupling strengths with a relative ratio of 1.4. The electron-phonon interactions are thus predicted to be of comparable strength for the two electronic transitions.

The coupled-mode eigenfrequencies can be calculated to a first approximation by using a phenomenological Hamiltonian of the form

$$\begin{pmatrix} E_1 & 0 & V_1 \\ 0 & E_2 & V_2 \\ V_1 & V_2 & E_p \end{pmatrix}, \quad (2)$$

which represents the coupling of two electronic excitations of energies  $E_1$  and  $E_2$  with a phonon of energy  $E_p = 310 \text{ cm}^{-1}$ ; the interaction potentials being  $V_1$  and  $V_2$ . Setting  $V_1/V_2 = 1.4$  and using as the eigenfrequencies of the coupled system the peak values observed in the data of Fig. 2 for  $T = 4.2 \text{ K}$ , we obtain  $E_1 = 277 \text{ cm}^{-1}$ ,  $E_2 = 301 \text{ cm}^{-1}$ ,  $V_1 = 37 \text{ cm}^{-1}$ , and  $V_2 = 24 \text{ cm}^{-1}$ . The predicted uncoupled electronic transition energies are close to those predicted in Ref. 16. The electron-phonon coupling strengths are, however, an order of magnitude larger than any others observed to date in a trivalent rare-earth electron-phonon coupled system.<sup>1-10</sup> The physical mechanism for this large coupling strength is still unknown. In transition-metal systems, where the electron-phonon coupling is significantly larger than in rare-earth doped systems, a similar coupling between an electronic excitation and  $E_g$  phonons has been proposed to explain observed anomalies in the Raman spectrum of  $\text{FeCl}_2$ .<sup>20</sup>

The electronic excitations should also appear in the electronic Raman spectra with  $\Gamma_1$ ,  $\Gamma_2$ ,  $\Gamma_3$ , and  $\Gamma_4$  symmetry. These symmetries correspond to the  $XY$ ,  $YX$ ,  $XX$ , and  $YY$  polarization combinations. In these symmetries, since no phonon is nearly degenerate with the electronic excitations, they will not be hybridized and hence uncoupled electronic excitations should be observed in the Raman spectra. The  $XY$  spectrum is shown in Fig. 3 and shows evidence of a broad feature in the 265–295- $\text{cm}^{-1}$  region (and perhaps another one around 300  $\text{cm}^{-1}$ ), due to the electronic transitions. The breadth of the lines makes the identification of the number of the transitions or their central frequency difficult. The values obtained above (277 and 301  $\text{cm}^{-1}$ ) are, however, consistent with the data of Fig. 3. Finally, one may observe in Fig. 3 that the electronic excitations have large linewidths—even at 4.2 K. These linewidths increase with temperature, and probably provide the main contribution to the anomalously large 50- $\text{cm}^{-1}$  width observed at room temperature for the broad line at 300  $\text{cm}^{-1}$ .

The present phenomenological approach can be pur-

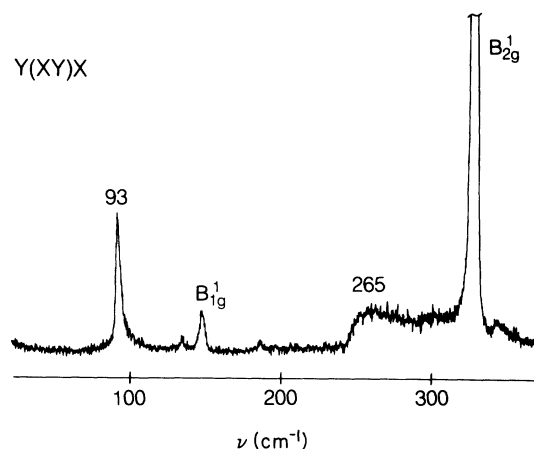


FIG. 3. Raman spectra of the crystal  $\text{YbPO}_4$  in the  $Y(XY)X$  configuration, at 4.2 K. The presence of phonon  $B_{1g}^1$  is due to slight leakage from the  $(XX)$  and  $(YY)$  polarizations, and  $B_{2g}^1$  is a strong phonon at 330  $\text{cm}^{-1}$  (Ref. 14). 256  $\text{cm}^{-1}$  is the estimated center of a broad transition that is presumably due to an electronic Raman transition. The line at 93  $\text{cm}^{-1}$  is an electronic Raman transition of  $\text{Yb}^{3+}$  to the first excited crystal-field state of its ground-state multiplet.

sued further to understand the temperature dependence of the spectra. At finite temperatures, all of the ytterbium ions are no longer in their ground state. When the ion is in a thermally excited state, the electronic Raman excitation originating in that state is no longer resonant with the  $E_g^3$  phonon at 310  $\text{cm}^{-1}$ , and the coupling is small. For a given ion, the electronic wave function is a superposition of the thermally accessible states in the ground-state multiplet, and the electron-phonon interaction potential has a thermal average which is given by  $\langle V \rangle = \text{Tr}(\rho V)$ , where  $\rho$  is the density matrix of the ion. Since only resonant excitations will be coupled,  $\langle V \rangle$  will be proportional to the electronic ground-state population factor.

The partition function is easily calculated from the four levels in the ground-state multiplet, with the main effect coming from the level at 93  $\text{cm}^{-1}$ .  $V_1$  and  $V_2$ , as determined above, were calculated as a function of temperature, producing new eigenfrequencies that are a function of temperature. Figure 4 shows

$$(\omega_{e2} - \omega_{e1})_T / (\omega_{e2} - \omega_{e1})_{T=4.2K},$$

the calculated and observed energy separation between the lowest and highest energy transitions in the 300- $\text{cm}^{-1}$  region, relative to that at  $T = 4.2 \text{ K}$ . The calculation was done for the three-level system for several different values of  $V_1/V_2$ . A calculation was also carried out for a two-level system and the result is also shown in Fig. 4. The agreement between the observed and calculated splittings is qualitatively quite good. The temperature at which the splitting starts decreasing significantly, 100 K, is the temperature at which  $kT$  becomes comparable to 93  $\text{cm}^{-1}$ . A more sophisticated calculation, using the Green's-function method, that takes into account the finite linewidths of the electronic excitations,<sup>21</sup> can be found in Ref. 14. A good fit to the experimental spectra at  $T = 4.2$

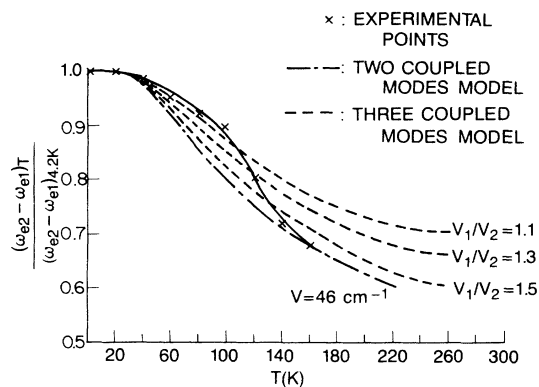


FIG. 4. Splitting of the coupled modes of  $\text{YbPO}_4$ , as a function of temperature, in  $\Gamma_5$  symmetry. Experimental and calculated curves are shown. The smooth curve drawn through the experimental points is a guide to the eye.

$K$  can be obtained using the parameters listed above with linewidths of 14 and  $37 \text{ cm}^{-1}$  for the two electronic transitions (not unreasonable given the broad lines visible in the  $XY$  spectrum).

In conclusion, results have been presented for the electronic Raman spectra of  $\text{YbPO}_4$ , with evidence for a very large temperature-dependent electron-phonon coupling

that has not been, to the authors' knowledge, observed for other rare-earth phosphate crystals. The symmetry characteristics of the coupling appear to be well understood and the temperature dependence of the splitting has been qualitatively explained. Clearly, more detailed work is needed to understand fully the coupling mechanisms and the reason why they are peculiar to  $\text{YbPO}_4$ . The application of a magnetic field would lift the degeneracy of the  $\Gamma_5$  excitations and presumably split the observed electronic Raman transitions. This approach could help to identify the electronic components of the lines. Finally, the spectra of the mixed crystals  $\text{Yb}_x\text{Lu}_{1-x}\text{PO}_4$ , reported in Ref. 14, may also shed some light on this problem.

We are extremely grateful to Dr. R. J. Elliott for illuminating discussions during the course of this work. We also thank R. E. Russo and J. J. Bucher for their expert technical assistance. The work performed at Lawrence Berkeley Laboratory was supported by the Director, Office of Energy Research, Office of Basic Energy Sciences, Chemical Sciences Division of the U.S. Department of Energy under Contract No. DE-AC03-76SF00098 and by the Division of Materials Science, U.S. Department of Energy, under Contract No. DE-AC05-84OR21400 with Martin Marietta Energy Systems, Inc.

\*Present address: AT&T Bell Laboratories, Murray Hill, NJ 07974.

†Present address: Naval Research Laboratories, Washington, D.C. 20375.

<sup>1</sup>M. Dahl and G. Schaack, *Phys. Rev. Lett.* **56**, 233 (1986).

<sup>2</sup>M. Gerlinger and G. Schaack, *Phys. Rev. B* **33**, 7438 (1986).

<sup>3</sup>W. Dorfler and G. Schaack, *Z. Phys. B* **59**, 283 (1985).

<sup>4</sup>W. Dorfler, H. D. Hochheimer, and G. Schaack, *Z. Phys. B* **51**, 153 (1983).

<sup>5</sup>K. Ahrens, H. Gerlinger, H. Lichtblau, G. Schaack, G. Abstreiter, and S. Mroczkowski, *J. Phys. C* **13**, 4545 (1980).

<sup>6</sup>K. Ahrens, *Z. Phys. B* **40**, 45 (1980).

<sup>7</sup>K. Ahrens and G. Schaack, *Phys. Rev. Lett.* **42**, 1488 (1979).

<sup>8</sup>G. Schaack, *Z. Phys. B* **26**, 49 (1977).

<sup>9</sup>P. Thalmeier and P. Fulde, *Z. Phys. B* **26**, 323 (1977).

<sup>10</sup>P. Thalmeier, *J. Phys. C* **17**, 4153 (1984).

<sup>11</sup>R. J. H. Clark and T. J. Dines, in *Advances in Infrared and Raman Spectroscopy*, edited by R. J. H. Clark and R. E. Hester (Heyden, London, 1982), Vol. 9, p. 282.

<sup>12</sup>P. C. Becker, N. Edelstein, G. M. Williams, J. J. Bucher, R.

E. Russo, J. A. Koningstein, L. A. Boatner, and M. M. Abraham, *Phys. Rev. B* **31**, 8102 (1985).

<sup>13</sup>P. C. Becker, N. Edelstein, B. R. Judd, R. C. Leavitt, and G. M. S. Lister, *J. Phys. C* **18**, L1063 (1985).

<sup>14</sup>P. C. Becker, Ph.D. thesis, University of California, Berkeley, 1986 (unpublished).

<sup>15</sup>T. Hayhurst, G. Shalimoff, N. Edelstein, L. A. Boatner, and M. M. Abraham, *J. Chem. Phys.* **74**, 5449 (1981).

<sup>16</sup>P. C. Becker, T. Hayhurst, G. Shalimoff, J. G. Conway, N. Edelstein, L. A. Boatner, and M. M. Abraham, *J. Chem. Phys.* **81**, 2872 (1984).

<sup>17</sup>R. J. Elliott, R. T. Harley, W. Hayes, and S. R. P. Smith, *Proc. Soc. London, Ser. A* **328**, 217 (1972).

<sup>18</sup>G. A. Gehring and K. A. Gehring, *Rep. Prog. Phys.* **38**, 1 (1975).

<sup>19</sup>R. J. Elliott (private communication).

<sup>20</sup>I. W. Johnstone, D. J. Lockwood, G. Mischler, J. R. Fletcher, and C. A. Bates, *J. Phys. C* **11**, 4425 (1978).

<sup>21</sup>J. F. Scott, *Phys. Rev. Lett.* **21**, 907 (1968).